

High-Density Surface EMG Decomposition based on a Convulsive Blind Source Separation Approach *

Xiangjun Zhu and Yingchun Zhang

Abstract—A novel automatic approach is developed in the present study to decompose high density surface electromyography (EMG) signals into motor unit (MU) firing patterns. The observed surface EMG signals are first modeled as a convulsive mixture of active MU sources. Contrast function maximization is employed to extract the first source, and separation of other sources is then carried out by an iterative deflation approach. Each extracted source is further processed and verified with the characteristics of motor unit action potential and firing patterns. The performance of the proposed automatic approach is evaluated in well-designed computer simulation. Results show that 4.7 ± 0.5 and 7.1 ± 0.6 MUs were correctly identified in the case of 5 and 10 active MUs respectively.

I. INTRODUCTION

The recently developed technique of high-density surface EMG (HD-sEMG) technology utilizes electrode grids over the skin surface to obtain detailed information of the underlying motor units (MUs) activities. HD-sEMG technology allows the noninvasive measure of motor unit properties which are difficult to assess with invasive technology, and is able to increase the number of detectable motor units with respect to selective intramuscular recordings [1]. Because of the low-pass filtering effect of the tissues and the limited selectivity of the recording systems, the surface EMG is classically analyzed as an interference signal. Therefore, decomposition of HD-sEMG, which separates constituent motor unit action potential (MUAP) trains from sEMG signals, is nontrivial.

Several methods have been developed for sEMG decomposition, such as template-matching techniques [2, 3], artificial intelligence algorithm [4], blind source separation (BSS) methods [5-7], and convolution kernel compensation (CKC) approach [8, 9]. Currently the BSS methods and CKC seem the most promising surface EMG decomposition methods since they do not rely on prior estimation of the shape and are not sensitive to the superimposition of action potentials [1]. Two mathematical models of the surface EMG mixing process, i.e., the instantaneous mixing model and convulsive mixing model, have been employed in the BSS methods. However, independent component analysis (ICA)

[5, 6] based on an instantaneous mixing model is not able to separate all the MUAP trains [10] due to shape variations and time delays between surface action potentials detected at different electrode locations. A blind source separation approach with a more advanced convulsive mixing model may be able to lead to superior performance.

In this study, a novel HD-sEMG decomposition method is developed based on the convulsive BSS. The new method models the surface EMG mixing process as a linear convulsive mixture, extracts the first source using the contrast optimization approach and employs an iterative deflation approach to estimate other MUAP trains.

II. METHODS

A. Model and problem formulation

The multichannel sEMG can be modeled as a multiple-input-multiple-output (MIMO) linear time invariant (LTI) system, which is a finite impulse response (FIR) filter with impulse response $((\mathbf{A}(n))_{n \in \mathbb{Z}})$ of length L [8]. Assuming a noise-free model, an M -dimensional discrete time sEMG signal $\mathbf{x}(n) = [x_1(n), \dots, x_M(n)]^T$ can be described as the convulsive mixture of the N -dimensional sources $\mathbf{s}(n) = [s_1(n), \dots, s_N(n)]^T$:

$$\mathbf{x}(n) = \sum_{l=0}^{L-1} \mathbf{A}(l)\mathbf{s}(n-l), \quad (1)$$

where $\mathbf{A}(l)$ is an $M \times N$ matrix which contains the l 'th mixing filter coefficients. In order to solve the separation problem blindly, the following assumptions on the characteristics of the sources are adopted: 1) $s_j(n), j \in \{1, \dots, N\}$ are stationary, zero-mean random processes with unit variance, and statistically mutually independent; 2) the number of sources must be less than or equal to the number of observed signals ($N \leq M$).

Recovering source signals from the observed signals only is equivalent to developing a MIMO-LTI inverse separating system, i.e., a separator [11, 12]. If the response of the separator is denoted by $((\mathbf{B}(n))_{n \in \mathbb{Z}})$, the separated outputs are then given by:

$$\mathbf{y}(n) = \sum_{k \in \mathbb{Z}} \mathbf{B}(k)\mathbf{x}(n-k). \quad (2)$$

*Research was supported in part by NIH K99DK082644 and 2011XZ009.

Xiangjun Zhu was with Zhijiang College, Zhejiang University of Technology, Hangzhou, China. He is now with the Department of Urology, University of Minnesota, Minneapolis, MN 55455 USA. (e-mail: zhux@umn.edu).

Yingchun Zhang is with the Department of Urology, University of Minnesota, Minneapolis, MN 55455 USA. (phone: 612-625-7939; fax: 612-626-0428; e-mail: zhang320@umn.edu).

In case of a successful separation, the components of $\mathbf{y}(n)$ hence correspond in any order to the components of $\mathbf{s}(n)$ up to a scalar filter. In an iterative deflation approach [11, 13], the separated output $\mathbf{y}(n)$ can be constructed component by component. A component $y(n)$ can be extracted by estimating the corresponding row of $\mathbf{B}(n)$:

$$y(n) = \sum_{k=0}^{K-1} \mathbf{b}(k) \mathbf{x}(n-k) = \sum_{i=1}^M \sum_{k=0}^{K-1} b_i(k) x_i(n-k), \quad (3)$$

where $b_i(k)$ represents the finite impulse response with length K of a causal separating filter.

B. Convolutional BSS in a deflation procedure

According to the assumptions on the sources described in the previous section, the source with the maximization of nongaussianity will be detected easily. Using kurtosis as a practical measure of nongaussianity, the extraction is achieved by maximizing a kurtosis contrast function:

$$J(\mathbf{b}(k)) = |kurt(y)|^2 = \left| \frac{E\{y(n)^4\}}{[E\{y(n)^2\}]^2} - 3 \right|^2, \quad (4)$$

where the kurtosis $kurt(y)$ is the fourth-order autocumulant of a separated component $y(n)$. A gradient algorithm is employed to maximize the contrast function [11]. At iteration $p \in \mathbb{N}$, we compute

$$\mathbf{y}^{(p)}(n) = (\mathbf{b}^{(p)} * \mathbf{x})(n) \quad (5)$$

$$\mathbf{b}^{(p+1)}(k) = \mathbf{b}^{(p)}(k) + \mu^{(p)} (\partial J(\mathbf{b}(k)) / \partial \mathbf{b}(k)), \quad (6)$$

where, $\mu^{(p)}$ is the step size, which can be determined optimally at each step; $\partial J(\mathbf{b}(k)) / \partial \mathbf{b}(k)$ is the gradient of the contrast function with respect to $\mathbf{b}(k)$.

After one of the sources (or a filtered version of it) is extracted, a so-called ‘‘deflation’’ method subtracts its contribution from the observed signals to obtain a mixture of $(N-1)$ sources [11]. This operation can be performed by a linear least square approach, and then the remaining problem amounts to separating $(N-1)$ sources from this reduced size mixture (whose size has been deflated). Repeating this procedure iteratively leads to the extraction of all the N sources. More precisely, we can subtract the contributions $\mathbf{z}^{(q-1)}(n)$ of the $(q-1)$ 'th source $y_{q-1}(n)$ from the corresponding mixture signals $\mathbf{x}^{(q-1)}(n)$ as follows

$$\mathbf{x}^{(q)}(n) = \mathbf{x}^{(q-1)}(n) - \mathbf{z}^{(q-1)}(n) \quad (7)$$

$$\mathbf{z}^{(q-1)}(n) = \sum_k \mathbf{t}^{(q)}(k) y_{q-1}(n-k), \quad (8)$$

where $(\mathbf{t}^{(q)}(k))_{k \in \mathbb{Z}}$ is the impulse response of a filter with L inputs and M outputs, which can be derived as a solution of a mean square linear estimation problem by minimizing

$$\varepsilon(\mathbf{t}^{(q)}) = E \{ |\mathbf{x}^{(q)}(n)|^2 \}. \quad (9)$$

C. HD-sEMG decomposition algorithm

Based on the convolutional mixture model and BSS method in a deflation approach, a novel algorithm is developed to decompose HD-sEMG into MU firing patterns. Fig. 1 shows a flowchart of the proposed algorithm.

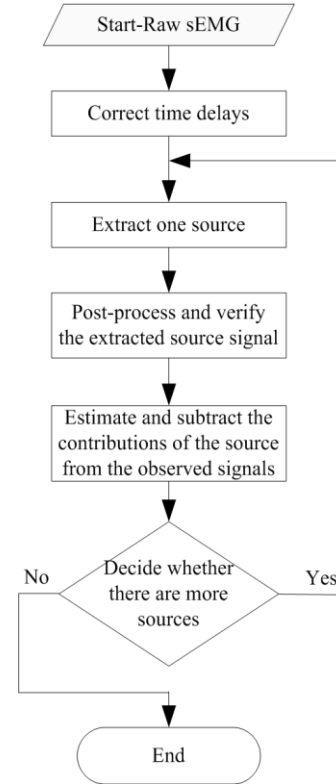


Figure 1. Flowchart of the high density sEMG decomposition algorithm

Time delay between signals at different electrodes along muscle fibers becomes significant in HD-sEMG recordings because of propagation of the intracellular potentials along muscle fibers. Cross-correlation of signals between consecutive channels along the muscle fibers is utilized to correct such time delays. A nonlinear energy operator (NEO) is employed to highlight the action potential peak, and then the NEO output is convolved with a Bartlett window to eliminate the spurious peaks due to background noise [14]. In this way, time delays are corrected and raw sEMG signals were aligned accurately by calculating the cross-correlation of the NEO filtered signals.

After time delay correction, the convolutional blind source separation algorithm with a deflation procedure (Section B) is employed to extract each MU from interference signals. The first source is firstly retrieved by calculating (5) and (6)

iteratively to maximize the kurtosis contrast function (4). The length of the causal separating filter $b_i(k)$ is set to 10.

The retrieved source signal is further post-processed to remove noise and to guarantee waveform similarity at each putative discharge time. Once the amplitude exceeds an adaptive threshold ($th=5 \times rms$, rms is the root-mean-square value), a peak is identified. Active segments which have a peak centered in a window of 10.5ms are suspected to contain MU activities and are retained. The similarity of active segments is calculated using the Euclidean distance, and a template is computed by averaging the active segments. The outlier segment which has dissimilar waveform with others is replaced with the template. Thus, the active segments in the source signal are homogeneity and more reliable particularly in case of superimposition.

The contributions of each retrieved source signal at all electrodes are estimated and subtracted from the observation signals according to (7)-(9). The recovered source signal is rechecked because of the effect of noise and the accumulation of estimation errors. If more than 5 peaks are detected in 1 sec in average, the recovered source is considered as a physiologically plausible MU source and its contribution is adopted as MUAP trains. If non valid MU source is recovered in three consecutive iterations, there is no further MU need to be identified. Otherwise, the convolutive BSS process is performed iteratively to extract sources from the updated observation signals.

III. RESULTS

A. Simulation of surface EMG

Synthetic surface EMG signals were generated using a planar volume conductor model [15] to test the performance of the proposed method. The volume conductor model consist of an anisotropic, semi-infinite muscle layer with a thickness of 10 mm, isotropic subcutaneous with a thickness of 3 mm and skin layer with a thickness of 1 mm. Parameters employed in the computer simulation are listed in the Tab. I. The intracellular action potential of a muscle fiber was modeled using a current tripole model [16]. A random number of fibers (uniformly distributed between 100 and 300) with the circular MU territories of 20 fibers/mm² was assumed in active MUs. Active MUs were also assumed with normally distributed conduction velocities (4.0 ± 0.3 m/s) and with the smallest MUs assigned the slowest conduction velocities. The MU firing patterns were represented by an inter-pulse interval (IPI) Gaussian distribution [17].

A surface EMG recording grid of 8×8 electrodes with 5-mm inter-electrode distance in both directions was assumed in the present study to record surface EMG signals. The center of the grid was placed at the center of the muscle. Surface EMG signals were sampled at a sampling frequency of 2000 Hz. Twenty simulations were performed by assuming 5 and 10 active MUs respectively. In each simulation, the position of the active MUs, numbers of fibers, conduction velocity, and discharging patterns were all randomly generated. Zero-mean Gaussian noise with signal-to-noise ratio (SNR) 15 and 20 dB was added to the simulated recordings, resulting 40 test signals for each number of active MUs.

TABLE I. PARAMETERS USED FOR SURFACE EMG SIMULATION

Parameter	Value
Conductivity of muscle(transverse)	0.1 S/m
Conductivity of muscle(longitudinal)	0.5 S/m
Conductivity of subcutaneous tissue	0.05 S/m
Conductivity of skin	0.1 S/m
Average half-fiber length	50 mm
Tendon ending spread	5mm
Innervation zone spread	5mm
Conduction velocity	4.0 ± 0.3 m/s
Mean IPI	90 ± 25 ms, range=[40...40ms]
IPI variation	10% of mean IPI
MU starting time	0 to mean IPI

B. Decomposition results

Fig.2 illustrates a typical decomposition result of 64 channel simulated sEMG signals (SNR=20dB) with the proposed convolutive BSS decomposition method. A portion of one channel signal is shown Fig.2 (a). The discharges of each identified MU are indicated by an assigned label at top of the signal. All the MU discharges can be correctly detected, especially when the number of superimposed potential actions is high at about 0.04s, 0.32s and 0.4s. The estimated MUAP templates and the true simulated waveforms are presented in Fig.2 (b).

Decomposition results of 80 simulated HD-sEMG signals are summarized in Tab. II. Each detected MU discharge is assumed to be identified correctly if it is within ± 2 samples from its true position. Only the MUs with over 90% correctly identified discharges are assumed to be identified. The deflation process is completed after 8 and 12 iterations on average in the case of 5 and 10 active MUs respectively. The results in Tab. II illustrate the number of identified MUs, average MU depth in muscle and average number of fibers of identified and missed MUs with respect to four test conditions. Most MUs (4.7 ± 0.5 and 7.1 ± 0.6 respectively) can be correctly identified in the case of 5 and 10 active MUs with 20dB SNR. Several MUs were missed because they were deeper in muscle tissue or had fewer fibers. The numbers of identified MUs decreased with increasing noise power and about half of the 10 active MUs were identified for 15dB SNR. On average, more than 93 ± 4 % of discharges were correctly detected for each identified MU.

As expected, the identification rate drops with the decreasing SNR and the increasing active MUs. The relative proportion of successfully identified motor units is generally related to motor-unit size and distance between the MUs and sEMG electrodes. The accumulation of estimation errors after several iterative deflation loops may become excessive. Therefore, some active MUs with weaken contribution to the recordings may be missed.

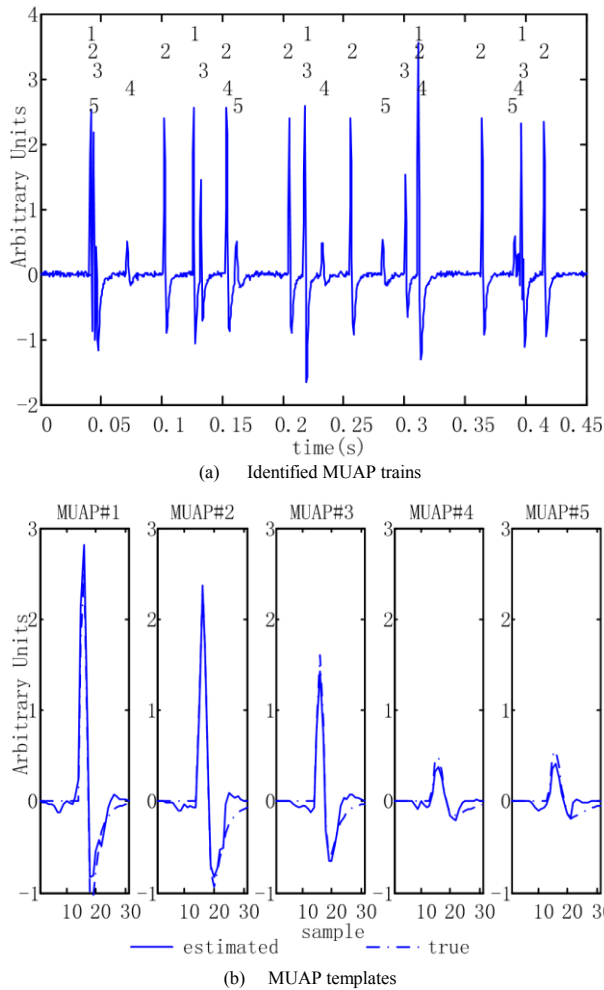


Figure 2. Decomposition example using convolutive BSS on synthetic SEMG signals.

TABLE II. DECOMPOSITION RESULTS ON SIMULATED SIGNALS

Number of simulated MUs and SNR(dB)	Average Number of identified MUs	Average depth in muscle		Average number of fibers	
		identified	missed	identified	missed
5	20	4.7±0.5	4.8±0.5	7.0±0.9	192±62
	15	3.7±0.5	4.2±0.6	6.4±1.0	199±65
10	20	7.1±0.6	4.1±1.4	7.1±1.0	197±70
	15	5.2±0.8	3.7±1.2	6.3±1.5	202±65

IV. CONCLUSION

An automatic high density surface EMG decomposition algorithm was successfully developed based on a convolutive blind source separation approach. Computer simulation shows that most active MUs can be correctly identified and the MUAP trains can be accurately reconstructed during lower-level contractions when there are not too much active MUs. The proposed algorithm also demonstrated the capability in satisfactorily solving superimpositions of MUAP trains.

ACKNOWLEDGMENT

This work was supported in part by K99DK082644 and the University of Minnesota Supercomputing Institute. The authors would also like to thank Dr. Jing Wang and Dr. Gerald Timm in the Department of Urology at the University of Minnesota Medical School for useful discussion.

REFERENCES

- [1] R. Merletti, A. Holobar and D. Farina, "Analysis of motor units with high-density surface electromyography," in *J. Electromyogr. Kinesiol.*, vol.18, pp. 879–890, 2008.
- [2] M. Gazzoni, D. Farina, and R. Merletti, "A new method for the extraction and classification of single motor unit action potentials from surface EMG signals," in *J. Neurosci. Meth.*, vol.136, pp.165–177, 2004.
- [3] B.U. Kleine, J. P. Dijk, B. G. Lapatki, et al., "Using two-dimensional spatial information in decomposition of surface EMG signals," in *J. Electromyogr. Kinesiol.*, vol.17, pp.535 – 548, 2007.
- [4] C. J. De Luca, A. Adam, R. P. Wotiz, et al., "Decomposition of surface EMG signals," in *J. Neurophysiol.*, vol.96, pp.2769–2774, 2006.
- [5] G. A. Garcia, R. Okuno and K. Akazawa, "A decomposition algorithm for surface electrode-array electromyogram—A noninvasive, three-step approach to analyze surface EMG signals," in *IEEE Eng. Med. Biol. Mag.*, vol.24, pp.63–72, 2005.
- [6] H. Nakamura, M. Yoshida, M. Kotani, et al., "The application of independent component analysis to the multi-channel surface electromyographic signals for separation of motor unit action potential trains: part I—measuring techniques," in *J. Electromyogr. Kinesiol.*, vol.14, pp.423–432, 2004.
- [7] A. Holobar and D. Zazula, "Correlation-based decomposition of surface electromyograms at low contraction forces," in *Med. Biol. Eng. Comput.*, vol.42, pp.487–495, 2004.
- [8] A. Holobar and D. Zazula, "Multichannel blind source separation using convolution kernel compensation," in *IEEE Trans. Sig. Process.*, vol.55, pp.4487–4496, 2007.
- [9] N. Jiang and D. Farina, "Covariance and time-scale methods for blind separation of delayed sources," in *IEEE Trans. Biomed. Eng.*, vol.58, no.3, pp.550–556, 2011.
- [10] P. Zhou, M. M. Lowery, and W.Z. Rymer, "Extracting motor unit firing information by independent component analysis of surface electromyogram: a preliminary study using a simulation approach", in *Int. J. Comp. Syst. Signals*, vol.7, pp.19–28, 2006.
- [11] C. Simon, Ph. Loubaton and C. Jutten, "Separation of a class of convolutive mixtures: a contrast function approach," in *Signal Processing*, vol.81, no.4, pp.883–887, 2001.
- [12] P. Comon and C. Jutten, *Handbook of Blind Source Separation: Independent component analysis and applications*. Academic Press, 2010, ch.8.
- [13] M.Castella, S.Rhioui, E. Moreau, et al., "Quadratic higher order criteria for iterative blind separation of a MIMO convolutive mixture of sources," in *IEEE Trans. Sig. Process.*, vol.55, no.1, pp.218–232, 2007.
- [14] H. Kim and J. Kim, "Neural spike sorting under nearly 0-dB signal-to-noise ratio using nonlinear energy operator and artificial neural-network classifier," in *IEEE Trans. Biomed. Eng.*, vol.47, no.10, pp.1406–1411, 2000.
- [15] D. Farina and R. Merletti, "A novel approach for precise simulation of the EMG signal detected by surface electrodes," in *IEEE Trans. Biomed. Eng.*, vol.48, no.6, pp.637–646, 2001.
- [16] R. Merletti and P. A. Parker. *Electromyography: Physiology, Engineering, and Non-invasive Applications*. New York: Wiley, 2004, ch.8.
- [17] J. Duchene and J. Y. Hogrel, "A model of EMG generation," in *IEEE Trans. Biomed. Eng.*, vol.47, no.2, pp.192–201, 2000.